nature geoscience

ARTICLES

https://doi.org/10.1038/s41561-018-0169-6

Deglacial floods in the Beaufort Sea preceded Younger Dryas cooling

L. D. Keigwin[1]*, S. Klotsko[2], N. Zhao[1], B. Reilly[3], L. Giosan[1] and N. W. Driscoll[2]

A period of cooling about 13,000 years ago interrupted about 2,000 years of deglacial warming. Known as the Younger Dryas (YD), the event is thought to have resulted from a slowdown of the Atlantic meridional overturning circulation in response to a sudden flood of Laurentide Ice Sheet meltwater that reached the Nordic Seas. Oxygen isotope evidence for a local source of meltwater to the open western North Atlantic from the Gulf of St Lawrence has been lacking. Here we report that the eastern Beaufort Sea contains the long-sought signal of ^{18}O-depleted water. Beginning at ~12.94 ± 0.15 thousand years ago, oxygen isotopes in the planktonic foraminifera from two sediment cores as well as sediment and seismic data indicate a flood of meltwater, ice and sediment to the Arctic via the Mackenzie River that lasted about 700 years. The minimum in the oxygen isotope ratios lasted ~130 years. We suggest that the floodwater travelled north along the Canadian Archipelago and then through the Fram Strait to the Nordic Seas, where freshening and freezing near sites of deep-water formation would have suppressed convection and caused the YD cooling by reducing the meridional overturning.

It is known that conditions in the Arctic Ocean have a profound effect on the North Atlantic Ocean, for example the Great Salinity Anomaly (GSA) of the 1960s and 1970s[1] and that the export of excess fresh water and ice through the Fram Strait was the origin of the GSA[2,3]. During the transit of the GSA around convective regions of the Nordic Seas, the decreased sea surface salinities and increased sea ice cover reduced the convective overturn and contributed to very harsh winters. There is reason to expect that similar and even larger climate events occurred in the past, especially during deglaciation when huge volumes of meltwater and ice suddenly entered the Gulf of Mexico, the Arctic and the Nordic Seas. For example, it was discovered several decades ago that an abrupt decrease in the oxygen isotope ratio ($\delta^{18}O$) in surface-dwelling planktonic foraminifera midway through deglaciation in the Gulf of Mexico was a signal of a freshwater flood[4]. The source of this runoff must have been the decaying Laurentide Ice Sheet (LIS) via the Mississippi River, but it ended abruptly at about 13 thousand years ago (ka) (ref. [5]). Kennett and Shackleton[4] proposed that, as the southern margin of the LIS retreated northward, meltwater was routed eastward to the Gulf of St Lawrence and the western North Atlantic. The $\delta^{18}O$ decrease in the Gulf of Mexico was more than 2‰, so a signal of 1‰ or more should stand out in fresher, higher latitude waters. However, a low $\delta^{18}O$ signal at about 13 ka has not been detected in high-quality sediment cores from the open western North Atlantic[6–8], and yet it is believed that the diversion of the flood from the Gulf of Mexico interrupted deep ocean convection and caused the well-known Younger Dryas (YD) cold episode (12.9–11.7 ka) in the North Atlantic region[9]. Other proposed explanations for the origin of the YD include melting of the Fennoscandian ice sheet[10], changes in atmospheric circulation[11] and a combination of ice-sheet melting, atmospheric flow patterns and radiative forcing[12]. However, these explanations beg the question as to where the diverted meltwater went.

The YD was discovered near the beginning of the 20th century as one of several appearances of the Arctic wildflower *Dryas octopetala* in postglacial deposits in Scandinavia[13,14] and eventually was defined as a useful chronostratigraphic zone in the North Atlantic region[15]. It was later proposed that meltwater-routing and drainage-pattern changes could have caused the YD by lowering the surface ocean salinity[16,17].

Recently, a glacial systems model showed that fresh water stored in the glacial Lake Agassiz most probably travelled north to the Beaufort Sea via the Mackenzie River at 13 ka (ref. [18]) and extensive field work on the Mackenzie Delta identified clear evidence of massive flood deposits that occurred at about the same time[19]. Although the exact timing and magnitude of the conclusions of Murton et al.[19] have been questioned[20], the application of a high-resolution ocean circulation model[21] showed that the Lake Agassiz flood could have caused the YD reduction of the Atlantic meridional overturning circulation (AMOC)[22] and consequent northern hemisphere cooling only when it was released to the Arctic Ocean (via the Mackenzie River).

Here we present data that show two events of substantial sea surface freshening during deglaciation in newly acquired large-diameter (jumbo) piston cores (JPCs) from 690 m on the continental slope ~100 km east of the Mackenzie River (JPC-15 and JCP-27 (Fig. 1)). These and other new cores underlie the Atlantic water that enters the Arctic at the Fram Strait and the Barents Sea in the depth range ~100 to 800 m and circulates anticlockwise along the continental slopes[23]. JPC-15 penetrated ~13 m of sediment and was probably stopped by a coarse ice-rafted debris (IRD) layer that has a high magnetic susceptibility, high Ca content (Fig. 2) and makes a prominent reflector in the acoustic stratigraphy across the region (Fig. 3). Later, reoccupying the same site, a longer (heavier) deployment (JPC-27) penetrated the deeper coarse layer. As these cores have nearly identical lithology, we spliced them together to make a composite JPC-15/27 (Supplementary Fig. 1).

Compared to the lower layer, the upper coarse layer at this site is thicker, has multiple events and fewer IRD grains (Fig. 2), but each layer also has finer sand and silt (Fig. 3). These data indicate that each coarse layer provides a record of enhanced sediment transport to the upper slope of the Beaufort Sea. The two main events must

[1]Woods Hole Oceanographic Institution, Woods Hole, MA, USA. [2]Scripps Institution of Oceanography, University of California San Diego, La Jolla, CA, USA. [3]College of Earth, Ocean, and Atmospheric Sciences, Oregon State University, Corvallis, OR, USA. *e-mail: lkeigwin@whoi.edu

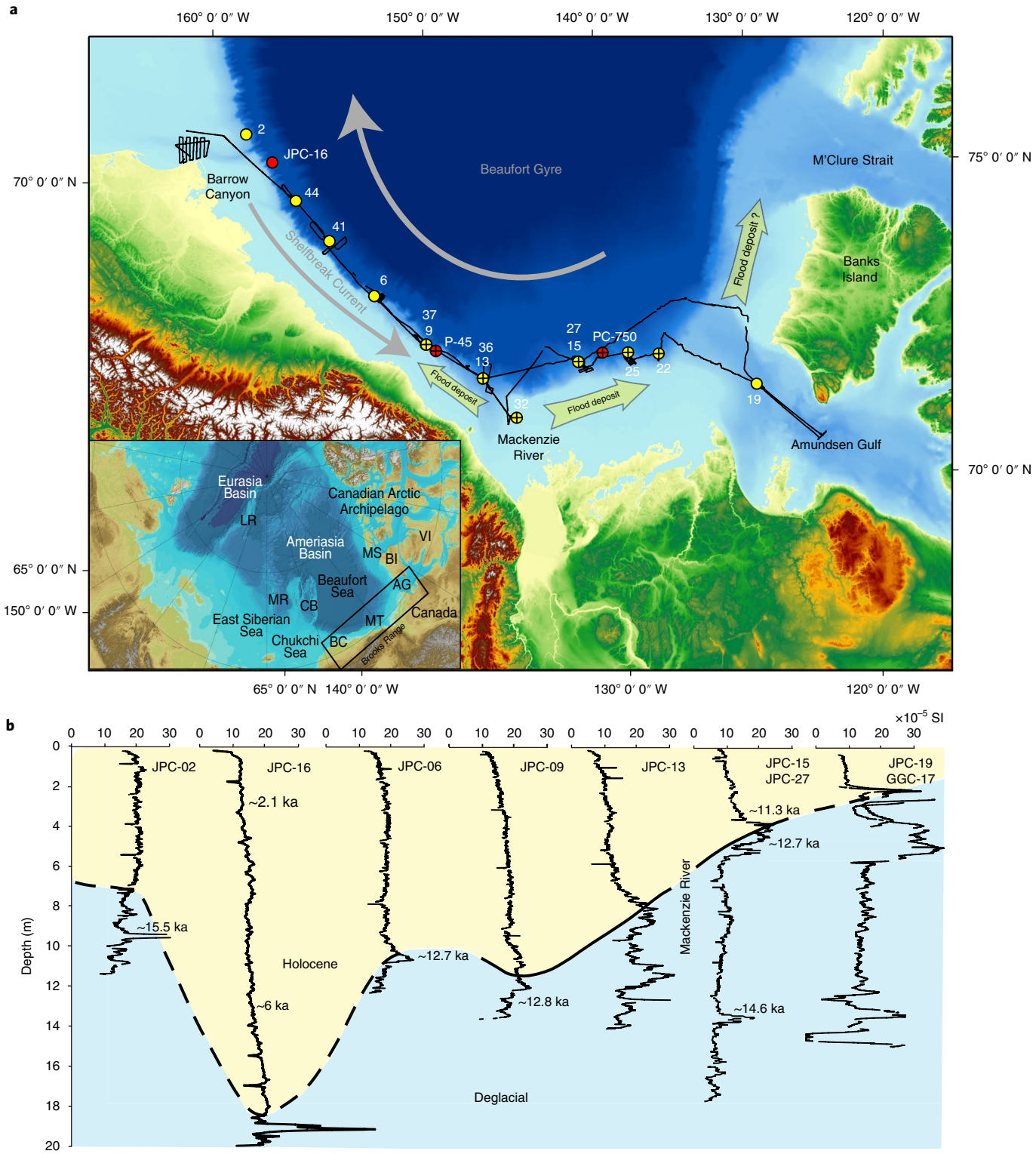

Fig. 1 | Overview of core locations and stratigraphy in the eastern Beaufort Sea. a, Track of USCGC Healy cruise 1302 (ref. [53]) with locations of JPC sites (yellow) and other cores (red) discussed in this study. The inset (based on data from Jakobsson et al.[53]) shows the study area with respect to the Arctic Ocean. LR, Lomonosov Ridge; MR, Mendeleev Ridge; CB, Chukchi Borderland; BC, Barrow Canyon; MT, Mackenzie Trough; AG, Amundsen Gulf; MS, M'Clure Strait; BI, Banks Island; VI, Victoria Island. Based on low $\delta^{18}O_{Nps}$ and seismic evidence, the YD flood deposit (sites in yellow with a cross) ranges from JPC-09 in the west to JPC-22 in the east. The Coriolis force and lowered sea level mean that the flood would have travelled north and east. **b**, Downcore magnetic susceptibility delineates the Holocene (yellow)–Deglacial (blue) boundary, and selected AMS ^{14}C dates are in calibrated ka.

be the same as those Scott et al.[24] noted in Canadian core PC-750 (Fig. 1). X-ray fluorescence (XRF) counts of calcium (interpreted as the detrital $CaCO_3$ content) show that our two events have a similar carbonate content, but also that the lowest carbonate delivery to the region occurred before the oldest event and was only a little higher between the events (Fig. 2). Sediment deeper than ~5 m is faintly

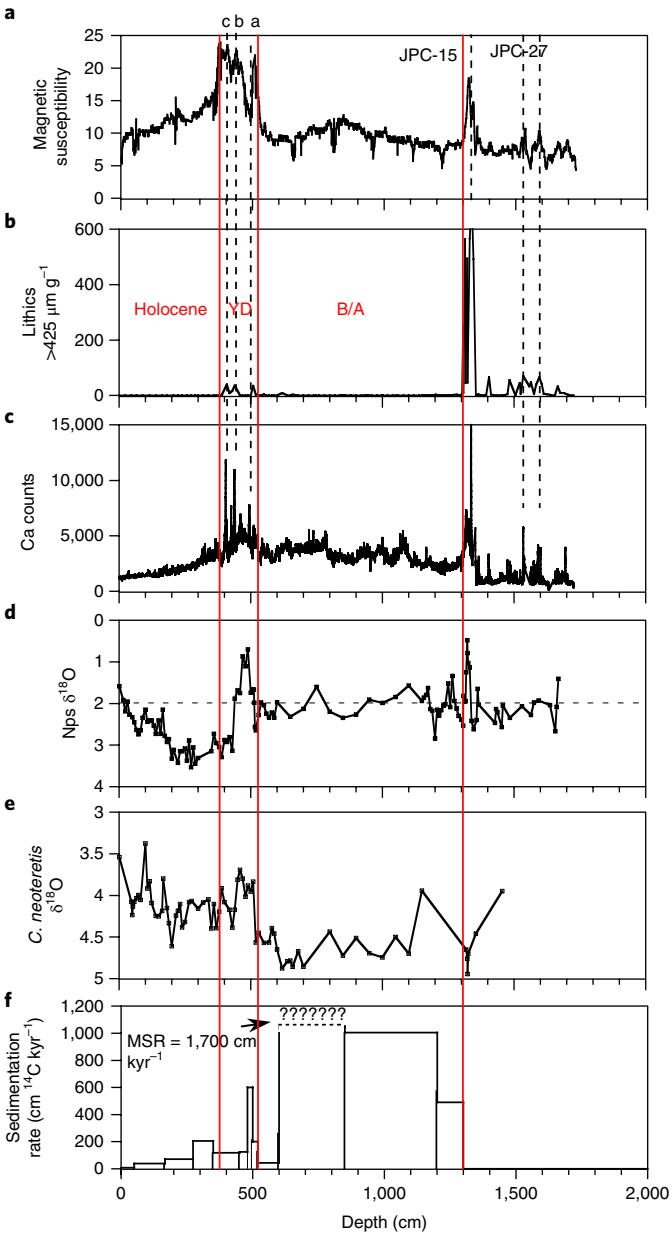

Fig. 2 | Proxy data from JPC-15/27 in the eastern Beaufort Sea. **a**–**d**, Magnetic susceptibility (**a**), lithic particle abundance (**b**), Ca content (proxy for $CaCO_3$) (**c**), and $\delta^{18}O_{Nps}$ (**d**) all exhibit extreme values early in the B/A warming at 14.6 ka (red line at 1,300 cm) and during the YD (11.7–12.9 ka) (red lines at ~380 and 510 cm). Dashed vertical lines correlate the smaller features. The dashed horizontal line in **d** is an ~2.0‰ reference for $\delta^{18}O$ features. Data that correspond to a large dropstone at 1,346–1,355 cm are excluded from **c**. **e**, The *C. neoteretis* (benthic) $\delta^{18}O$ is unremarkable except that the clear minimum of ~450–500 cm occurs in the same samples as the low $\delta^{18}O_{Nps}$. **f**, Sedimentation rates are very high where sediments are laminated, although ^{14}C dates exaggerate the B/A maxima (Supplementary Fig. 2). MSR, minimum sedimentation rate.

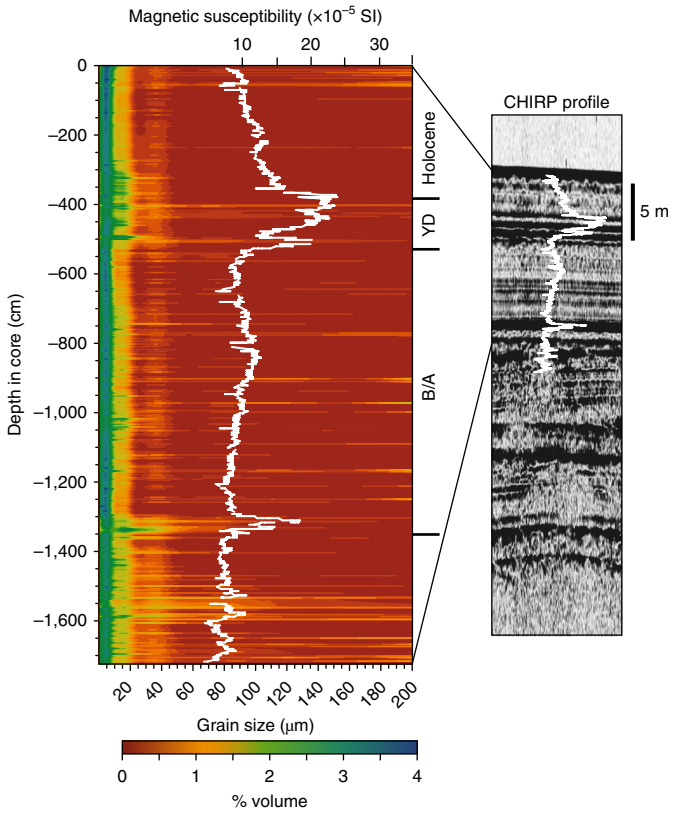

Fig. 3 | Grain size variability down composite JPC-15/27. Magnetic susceptibility data are superposed on the grain size and the seismic data, assuming the pressure-wave velocity of the core logged at sea (1,333 m s^{-1}). These properties all vary together. The seismic data show a diagnostic reflector pattern with upper (~380–520 cm) and lower high (~1,320 cm) amplitude reflectors that bound a region of lower acoustic reflectivity. The zone of lower reflectivity correlates with high sediment accumulation rates, low magnetic susceptibility, low IRD and low Ca content (Fig. 2).

laminated at the centimetre scale, except for the massive appearance of the first event (13.0–13.5 m). Laminae are better developed between 6 and 12 m, where about 300 were counted in the XRF data (Supplementary Fig. 2).

As with the sediment and geophysical data, $\delta^{18}O$ on the polar planktonic foraminifer *Neogloboquadrina pachyderma* (Ehrenberg) left coiling (Nps (s, sinistral)) in JPC-15/27 is marked by two prominent events at the same depths in the core (Fig. 2). At these levels, $\delta^{18}O$ of Nps ($\delta^{18}O_{Nps}$) decreased at least 1.0‰ below the ~2.0‰ baseline that extends >4 m down the core. Above a pronounced maximum in $\delta^{18}O_{Nps}$ at 2–3 m, values decrease by ~2.0‰ to the core top. We find the upper $\delta^{18}O_{Nps}$ minimum to the west of JPC-15/27 at JPC-09 (Supplementary Information), but not at other cores farther west (Fig. 1). Benthic foraminiferal (*Cassidulina neoteretis* Seidenkrantz) $\delta^{18}O$ at JPC-15/27 yields a stratigraphy more typical of the world ocean, with generally increasing values down the core, although they are consistently low at about 5 m in the same samples in which $\delta^{18}O_{Nps}$ is low (Fig. 2e).

Chronology

The chronology in Arctic sediments is uncertain because, although radiocarbon dating of foraminifera is the simplest method, at present there is no way to know exactly the near surface reservoir correction (ΔR) in the past. We made 14 accelerator mass spectrometer (AMS) ^{14}C measurements on Nps from core 15 (Supplementary Table 1). These dates indicate maximum rates of sedimentation of at least 10 m per 1,000 ^{14}C years between 6 and 12 m in the mid-deglacial interval of the core (Fig. 2f and Supplementary Fig. 3). Before and after that mid-core extreme, rates are half that or less. We assume that Nps calcified near the interface between fresher, near-surface water and the underlying saltier water, as it does today[25]. In that environment, it was salty enough to survive, but shallow enough to capture low $\delta^{18}O$ events. Six of the Nps dates were paired with dates on *C. neoteretis*.

On average, benthics are only 120 ± 220 years older than planktonics, which includes a result from 1,300 m in the Chukchi Sea (HLY0205 JPC-16 (Fig. 1))[26]. This small difference indicates that the upper slope waters were relatively well ventilated.

For a calendar (calibrated) ^{14}C chronology, we need to choose a ΔR. In the modern Arctic, the Pacific inflow through Bering Strait is a source of old carbon that would have been absent prior to about 11 ka when the strait was dry land[26,27] (Supplementary Fig. 4 for further discussion). Bondevik et al.[28] showed that surface waters along the Norwegian coast, which would have fed the Arctic, had a ΔR of about 0 years, like today, during the Bølling-Allerød (B/A) and of about 100 years early in the YD and about 200 years during the mid-YD. Cao et al.[29] reached a similar conclusion based on U series dates and ^{14}C measurements on a solitary coral from the southern Labrador Sea, which would monitor intermediate-depth waters that leave the Nordic Seas. Therefore, we developed an age model using a Bayesian method and $\Delta R = 0 \pm 100$ years for the Holocene and the Allerød, and 200 ± 100 years for the YD (Supplementary Fig. 5). If the relatively high ΔR during the YD was triggered by an event late in the Allerød, then the onset of that event should be calibrated with a ΔR of ~0 years.

These estimates of only a modest ΔR (0–200 years) encompass the pre-bomb estimate[30] based on ^{14}C, tritium and $\delta^{18}O$ on samples collected decades ago when bomb-produced nuclides were beginning to invade the deep Arctic. Ostlund et al.[30] inferred that the pre-bomb ^{14}C activity of waters between 500 and 1,500 m was about -55 ± 5‰, to give a ΔR of ~40 years (Fig. 4). Therefore, although deep-water ^{14}C circulation in the Arctic may have been very different in the past[31,32], it appears that the ^{14}C ventilation of upper waters (<1500 m) in the Canada Basin was similar to today.

Our age model gives interpolated calendar ages in JPC-15/27 of 12.94 ± 0.15 ka for the onset of the upper $\delta^{18}O$ minimum (constrained by dates of 13.06 ka at 520 cm and 12.66 ka at 500 cm (Supplementary Table 1), and ~14.6 ka for the peak of the older one (Fig. 5). The age of the older event and its associated IRD is consistent with the ages (15.2–14.1 ka) reported for the initial withdrawal of ice streams from Amundsen Gulf and M'Clure Strait[33]. The age for the onset of the later freshening in the Beaufort Sea (12.94 ± 0.15 ka) is virtually the same as the beginning of the YD at 12.85 ± 0.14 ka in Greenland ice cores[34], and identical to the end of freshening in the Gulf of Mexico (12.94 ± 0.17 ka) (Fig. 5). Minimum $\delta^{18}O$ in JPC-15/27 first occurred at 12.59 ± 0.14 ka, within the uncertainty of the equivalent event at JPC-09 (12.7 ± 0.10 ka). The coincidence of the end of flooding in the Gulf of Mexico and the onset of flooding in the eastern Beaufort Sea is strongly suggestive that the routing of meltwaters[35] switched from the Gulf of Mexico to the Beaufort Sea at about 13 ka.

Ocean and climate change in the Beaufort Sea

Our composite sequence from the continental slope east of the Mackenzie River began around 15–16 ka with modest ice rafting from local sources, such as ice streams in M'Clure Strait and Amundsen Gulf. Icebergs would have travelled clockwise around the Canada Basin via the Beaufort Gyre, and the anticlockwise shelf-break current[36] would have been weakened with the sea level below the depth of the Bering Strait. Mackenzie River may not have supplied substantial detrital carbonate because the extensive Devonian carbonate terrain south of Great Slave Lake and north of Fort McMurray[37] was probably ice covered, but it

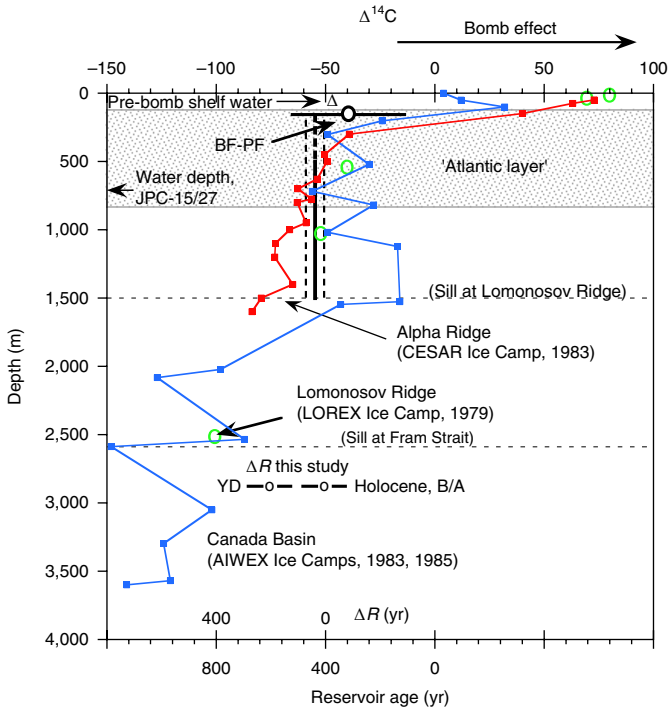

Fig. 4 | Radiocarbon basis for the age model in this paper. Ostlund et al.[30] synthesized $\Delta^{14}C$, $\delta^{18}O$ and tritium data collected from several Arctic ice camps (LOREX, CESAR and AIWEX) between 1977 and 1985 and concluded that the pre-bomb value of intermediate depth waters (500 to 1,500 m) was -55 ± 5‰ (vertical black line $\pm 1\sigma$ (dashed)), and pre-bomb shelf water was -48 ± 3‰ (triangle). The ice-camp results are considered to be equivalent to Canada Basin water in that all are on the west side of the Lomonosov Ridge. Our age model uses $\Delta R = 0 \pm 100$ (1σ) for the Holocene and B/A, within uncertainty of the pre-bomb estimate[30], but we use a larger ΔR for the YD (200 ± 100) (Supplementary Fig. 5).

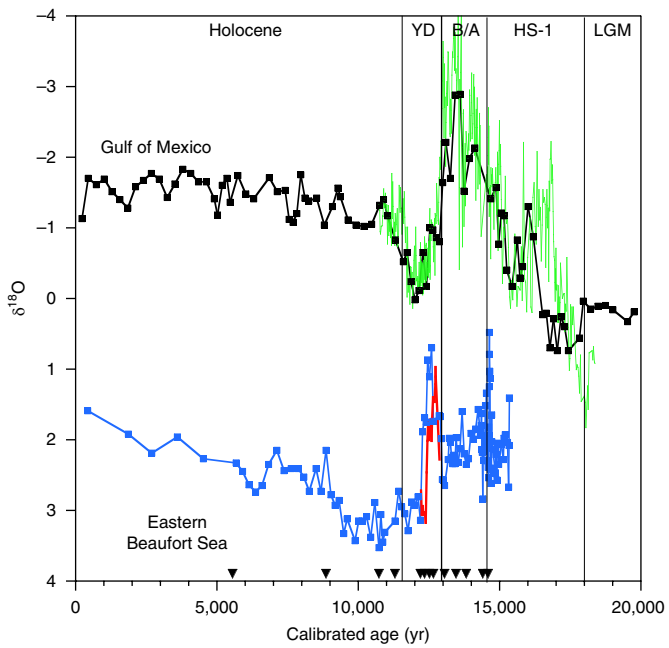

Fig. 5 | Comparison of deglacial $\delta^{18}O$ between Orca Basin in the Gulf of Mexico and Beaufort Sea. Arctic data are based on Nps (blue squares, core 15/27; red line, JPC-09) and Orca Basin data are based on the planktonic foraminifer *Globigerinoides ruber* (data from Williams et al.[5] (green line) and Leventer et al.[54] (black squares) (Supplementary Information gives chronology details of the latter core)). The eastern Beaufort Sea freshened at about 12.9 ka, coincident with the end of the Gulf of Mexico freshening and consistent with the hypothesis that meltwater was diverted from the Gulf to a more northern outlet as deglaciation progressed[4]. HS-1, Heinrich Stadial 1; LGM, last glacial maximum.

may have been a source of runoff and sediment at least since ~18 ka based on the background low $\delta^{18}O$ (Fig. 5). This was a time when the secular change in the ocean due to increased ice volume was about +1‰, which indicates that the sea surface was less saline than today by at least one practical salinity unit, assuming the modern $\delta^{18}O$–salinity relationship[38]. This setting prevailed until ~14.6 ka, when ice rafting dramatically increased from the Amundsen Gulf and M'Clure Strait, and $\delta^{18}O_{Nps}$ decreased by >1‰. The five samples that define this minimum were probably deposited within decades.

At the end of the 14.6 ka event, the Amundsen Gulf probably remained a source of sediment to the continental slope in the eastern Beaufort Sea until the ice stream had fully retreated. Mackenzie River may have always been a large source of sediment, but as more of its watershed north of Fort McMurray was deglaciated, the more important it must have become. The laminated sediments, high sedimentation rate and general lack of coarse particle ice rafting suggest a large sediment input from the Mackenzie River between 13.5 and ~14.4 ka (6–12 m in the core). The high sedimentation rates along the slope may be explained by discharge over bottom fast ice on the shelf, which could efficiently transport sediment farther seaward (for example, Macdonald and Yu[39]). Based on the diagnostic acoustic signature of the rapidly emplaced B/A section (Fig. 3), the western extent of the deposit pinches out between JPC-09 and JPC-06 (Fig. 1 and Supplementary Fig. 8). Counts of ~300 layers within the ~900 year interval during which sedimentation rates were highest show that the layers were probably not annual (Supplementary Fig. 2). The interval between the two $\delta^{18}O_{Nps}$ minima represents most of the B/A climate warming, when the AMOC was almost as strong as today[22], but evidently the lowered salinity in the Beaufort Gyre had little direct influence on North Atlantic overturning. This may indicate that the gyre was in a mostly anticyclonic state, which today stores ice and fresh water[40].

Close to 13 ka, the rapid increase in magnetic susceptibility and decreased $\delta^{18}O_{Nps}$ in JPC-15/27 heralded the beginning of the YD. Although the two $\delta^{18}O_{Nps}$ minima in this core are similar in size, the YD event was more likely to have been a flood of fresh water with a high suspended load[19] because $\delta^{18}O$ of *C. neoteretis*, living at the seafloor, decreased in exactly the same samples as Nps during the ~13 ka event, but not the earlier event. This, we propose, may record a hyperpycnal flow that brought low salinity to the seafloor and that would be more likely from a river flood. The major sediment depocentre in this model must be farther seaward because sedimentation rates drop during this time interval at 690 m water depth (Fig. 2). The YD flood can be traced to the west as far as core JPC-09 using $\delta^{18}O_{Nps}$, but the signal is not clear west of that at JPC-06, and neither the $\delta^{18}O$ minima nor the maximum in magnetic susceptibility are evident as far west as JPC-02 near Barrow, Alaska (Supplementary Fig. 7).

About 200 years after the onset of the YD flood, all four sediment and isotope proxies were briefly aligned in the first (labelled 'a' in Fig. 2) of several subevents (Fig. 2a–d). The low $\delta^{18}O_{Nps}$ episode is mostly centred between the subpeaks 'a' and 'b' of the magnetic susceptibility (12.8 to 12.3 ka), but the last of the spikes in IRD and carbonate deposition ended with an increased $\delta^{18}O_{Nps}$ at the end of the flooding. The maximum $\delta^{18}O_{Nps}$ at ~12.2 ka probably marks an interval of relatively high salinity in the near-surface Beaufort Sea[41], followed by more typical decreasing $\delta^{18}O$ trends in benthic and planktonic foraminifera as the ice volume decreased and climate warmed during the Holocene. The lingering high magnetic susceptibility late in the YD may indicate evolving sources of sediment from the Mackenzie River, and it might also relate to evidence of a second flood ~11 ka (ref. [19]).

Knowing the duration of the YD flood is important to calculate the fresh-water transport and evaluate its effect on the AMOC. If we take the main flood interval of the YD as that part during which $\delta^{18}O_{Nps}$ was less than the 2‰ baseline, then it lasted ~660 years. If the lowest $\delta^{18}O_{Nps}$ indicates the peak discharge, then most of the fresh-water transport could have occurred in about 130 years (Supplementary Table 3). However, it must be kept in mind that if the Mackenzie River choke point at Fort McMurray was breached suddenly at the beginning of the YD, and this is contentious[42], then the outburst of Glacial Lake Agassiz water would have probably produced initial salinities over our core site that were too low for Nps to grow. Furthermore, estimates of very high fresh-water transport during the flood are based on the assumption that it occurred on the timescale of a year[43], yet if the main flood was that brief then it is unlikely that enough planktonic foraminifera could have recorded the low $\delta^{18}O$ to leave a signal in the geological record.

Most probably, the initial Mackenzie discharge at 12.9 ka was a combination of both a routing change from the Gulf of Mexico and an outburst flood from the glacial Lake Agassiz. This potent combination of two sources of fresh water was probably effective in reducing the AMOC[35], especially given that it was an Arctic source[21]. However, even if the combined routing plus glacial lake release to the Mackenzie River itself was too modest to trigger a collapse of the AMOC, many large rivers empty into the Arctic[2], and the Lena River, one of the largest, also flooded about 13 ka (ref. [44]). Finally, in addition to fresh-water floods in the Arctic around the beginning of the YD, it is reported that an enhanced sea-ice export through the Fram Strait at that time also had a Beaufort Sea source[45].

By the onset of the YD, the AMOC may have already been close to a tipping point after ~1,500 years of low salinity leakage from the Beaufort Sea and transport to the nearshore convective regions of the Nordic seas[46,47]. Increased freshening has also been noted at other coastal locations in the North Atlantic, including the proposed eastern outlet (St Lawrence River system) using various proxies[48–50], the Baltic Sea[10,51] and off eastern Greenland, where $\delta^{18}O_{Nps}$ minima of YD age are thought to reflect local melting[52] but could also be evidence of the Mackenzie flood. The coincidence of decreased $\delta^{18}O$ in the Beaufort Sea and increased $\delta^{18}O$ in the Gulf of Mexico near the beginning of the YD is a good test of the meltwater-diversion hypothesis of Kennett and Shackleton[4] (Fig. 5). Given all the other observations, which include the climatic background suggested by alternative hypotheses[10–12] that may have helped sustained the event, and the lack of a large YD minimum in $\delta^{18}O$ anywhere in the open North Atlantic Ocean, the ~12.9 ka flood of the Mackenzie River was most probably the trigger for the reduction of the AMOC and YD cooling.

Methods

Methods, including statements of data availability and any associated accession codes and references, are available at https://doi.org/10.1038/s41561-018-0169-6.

Received: 31 October 2017; Accepted: 29 May 2018;
Published online: 09 July 2018

References

1. Dickson, R. R., Meincke, J., Malmberg, S. A. & Lee, A. J. The 'Great Salinity Anomaly' in the Northern North Atlantic 1968–1982. *Prog. Oceanogr.* **20**, 103–151 (1988).
2. Aagard, K. & Carmack, E. The role of sea ice and other fresh water in the Arctic circulation. *J. Geophys. Res.* **94**, 14485–14498 (1989).
3. Häkkinen, S. An Arctic source for the great salinity anomaly: a simulation of the Arctic ice-ocean system for 1955-1975. *J. Geophys. Res.* **98**, 16397–16410 (1993).
4. Kennett, J. P. & Shackleton, N. J. Laurentide ice sheet meltwater recorded in Gulf of Mexico deep-sea cores. *Science* **188**, 147–150 (1975).
5. Williams, C., Flower, B. & Hastings, D. W. Seasonal Laurentide ice sheet melting during the 'Mystery Interval' (17.5–14.5 ka). *Geology* **40**, 955–958 (2012).

6. Keigwin, L. D. & Jones, G. A. The marine record of deglaciation from the continental margin off Nova Scotia. *Paleoceanography* **10**, 973–985 (1995).
7. de Vernal, A., Hillaire-Marcel, C. & Bilodeau, G. Reduced meltwater outflow from the Laurentide ice margin during the Younger Dryas. *Nature* **381**, 774–777 (1996).
8. Keigwin, L. D., Sachs, J., Rosenthal, Y. and Boyle, E. A. The 8200 year B.P. event in the slope water system, western subpolar North Atlantic. *Paleoceanography* **20**, PA2003 (2005).
9. Broecker, W. S. et al. The routing of meltwater from the Laurentide ice-sheet during the Younger Dryas cold episode. *Nature* **341**, 318–321 (1989).
10. Muschitiello, F. et al. Fennoscandian freshwater control on Greenland hydroclimate shifts at the onset of the Younger Dryas. *Nat. Commun.* **6**, 8939 (2015).
11. Brauer, A. et al. An abrupt wind shift in western Europe at the onset of the Younger Dryas cold period. *Nat. Geosci.* **1**, 520–523 (2008).
12. Renssen, H. et al. Multiple causes of the Younger Dryas cold period. *Nat. Geosci.* **8**, 946–950 (2015).
13. Andersson, G. *Swedish Vegetation History* (P.A. Norstedt & Soners, Stockholm, 1897).
14. Hartz, N. & Milthers, V. The late glacial clay in the Allerod brickyard. *Medd. Dan. Geol. Foren.* **8**, 31–60 (1901).
15. Mangerud, J., Andersen, S. T., Berglund, B. E. & Donner, J. J. Quaternary stratigraphy of Norden, a proposal for terminology and classification. *Boreas* **3**, 110–127 (1974).
16. Johnson, R. G. & McClure, B. T. A model for northern hemisphere continental ice sheet variation. *Quat. Res.* **6**, 325–353 (1976).
17. Rooth, C. Hydrology and ocean circulation. *Prog. Oceanogr.* **11**, 131–149 (1982).
18. Tarasov, L. & Peltier, W. R. Arctic freshwater forcing of the Younger Dryas cold reversal. *Nature* **435**, 662–665 (2005).
19. Murton, J. B., Bateman, M. D., Dallimore, S. R., Teller, J. T. & Yang, Z. Identification of Younger Dryas outburst flood path from Lake Agassiz to the Arctic Ocean. *Nature* **464**, 740–743 (2010).
20. Carlson, A. E. & Clark, P. U. Ice sheet sources of sea level rise and freshwater discharge during the last deglaciation. *Rev. Geophys.* **50**, RG4007 (2012).
21. Condron, A. & Winsor, P. Meltwater routing and the Younger Dryas. *Proc. Natl Acad. Sci. USA* **109**, 19928–19933 (2012).
22. McManus, J. F. et al. Collapse and rapid resumption of Atlantic meridional circulation linked to deglacial climate changes. *Nature* **428**, 834–837 (2004).
23. Rudels, B., Jones, E. P., Anderson, L. G. & Kaattner, G. On the intermediate depth waters of the Arctic Ocean. *Geophys. Monogr.* **85**, 33–46 (1994).
24. Scott, D., Schell, T., St-Onge, G., Rochon, A. & Blasco, S. Foraminiferal assemblage changes over the last 15,000 years on the Mackenzie–Beaufort Sea slope and Amundsen Gulf, Canada: implications for past sea ice conditions. *Paleoceanography* **24**, PA2219 (2009).
25. Bauch, D., Carstens, J. & Wefer, G. Oxygen isotope composition of living *Neogloboquadrina pachyderma* (sin.) in the Arctic Ocean. *Earth Planet. Sci. Lett.* **146**, 47–58 (1997).
26. Keigwin, L. D. et al. Flooding of Bering Strait and Holocene climate in the Chukchi Sea. *Geology* **34**, 861–864 (2006).
27. Jakobsson, M. et al. Post-glacial flooding of the Beringia Land Bridge dated to 11,000 cal yrs BP based on new geophysical and sediment records. *Clim. Past.* **13**, 991–1005 (2017).
28. Bondevik, S., Mangerud, J., Birks, H. H., Gulliksen, S. & Reimer, P. Changes in North Atlantic radiocarbon reservoir ages during the Allerod and Younger Dryas. *Science* **312**, 1514–1517 (2006).
29. Cao, L., Fairbanks, R. G., Mortlock, R. A. & Risk, M. A. Radiocarbon reservoir age of high latitude North Atlantic surface water during the last deglacial. *Quat. Sci. Rev.* **26**, 732–742 (2007).
30. Ostlund, H., Possnert, G. & Swift, J. Ventilation rate of the deep Arctic Ocean from carbon 14 data. *J. Geophys. Res.* **92**, 3769–3777 (1987).
31. Cronin, T. et al. Deep Arctic Ocean warming during the last glacial cycle. *Nat. Geosci.* **5**, 631–634 (2012).
32. Thornalley, D. J. R. et al. A warm and poorly ventilated deep Arctic Mediterranean during the last glacial period. *Science* **349**, 706–710 (2015).
33. Stokes, C. R., Clark, C. D. & Storrar, R. Major changes in ice stream dynamics during deglaciation of the north-western margin of the Laurentide ice sheet. *Quat. Sci. Rev.* **28**, 721–738 (2009).
34. Rasmussen, S. et al. A new Greenland ice core chronology for the last glacial termination. *J. Geophys. Res* **111**, D06102 (2006).
35. Meissner, K. & Clark, P. Impact of floods versus routing events on the thermohaline circulation. *Geophys. Res. Lett.* **33**, L1570 (2006).
36. von Appen, W.-J. & Pickart, R. Two configurations of the western Arctic Shelfbreak Current in summer. *J. Phys. Oceanogr.* **42**, 329–351 (2012).
37. Wheeler, J. et al. *Geological Map of Canada. "A" Series Map 1860A* (Geological Survey of Canada, 1996); https://doi.org/10.4095/208175
38. Cooper, L. et al. Linkages among runoff, dissolved organic carbon, and the stable oxygen isotope composition of seawater and other water mass indicators in the Arctic Ocean. *J. Geophys. Res.* **110**, G02013 (2005).
39. Macdonald, R. & Yu, Y. in *Estuaries* (ed. Wangersky, P. J.) 91–120 (Springer, Berlin, 2006).
40. Proshutinsky, A. & Johnson, M. A. Two circulation regimes of the wind-driven Arctic Ocean. *J. Geophys. Res.* **102**, 12493–12514 (1997).
41. Schell, T., Scott, D. B., Rochon, A. & Blasco, S. Late Quaternary paleoceanography and paleo-sea ice conditions in the Mackenzie Trough and Canyon, Beaufort Sea. *Can. J. Earth Sci.* **45**, 1399–1415 (2008).
42. Fisher, T. G., Waterson, N., Lowell, T. V. & Hajdas, I. Deglaciation ages and meltwater routing in the Fort McMurray region, northeastern Alberta and northwestern Saskatchewan, Canada. *Quat. Sci. Rev.* **28**, 1608–1624 (2009).
43. Leverington, D. W., Mann, J. D. & Teller, J. T. Changes in the bathymetry and volume of glacial Lake Agassiz between 11,000 and 9300 ^{14}C yr B.P. *Quat. Res.* **54**, 174–181 (2000).
44. Spielhagen, R. F., Erlenkeuser, H. & Siegert, C. History of freshwater runoff across the Laptev Sea (Arctic) during the last deglaciation. *Glob. Planet. Change* **48**, 187–207 (2005).
45. Hillaire-Marcel, C., Maccali, J., Not, C. & Poirier, A. Geochemical and isotopic tracers of Arctic sea ice sources and export with special attention to the Younger Dryas interval. *Quat. Sci. Rev.* **79**, 184–190 (2013).
46. Mauritzen, C. Production of dense overflow waters feeding the North Atlantic across the Greenland-Scotland Ridge. Part 1: evidence for a revised circulation scheme. *Deep-Sea Res.* **43**, 769–806 (1996).
47. Pedlosky, J. & Spall, M. Boundary intensification of vertical velocity in a beta-plane basin. *J. Phys. Oceanogr.* **35**, 2487–2500 (2005).
48. Carlson, A. E. et al. Geochemical proxies of North American freshwater routing during the Younger Dryas cold event. *Proc. Natl Acad. Sci. USA* **104**, 6556–6561 (2007).
49. Cronin, T. M., Rayburn, J. A., Guilbault, J.-P. & Thunell, R. Stable isotope evidence for glacial lake drainage through the St. Lawerence estuary, eastern Canada, ~13.1–12.9 ka. *Quat. Int.* **260**, 55–65 (2012).
50. Levac, E., Lewis, M., Stretch, V., Duchesne, K. & Neulieb, T. Evidence for meltwater drainage via the St. Lawrence River valley in marine cores from the Laurentian Channel at the time of the Younger Dryas. *Glob. Planet. Change* **130**, 47–65 (2015).
51. Boden, P., Fairbanks, R. G., Wright, J. D. & Burckle, L. H. High-resolution stable isotope records from southwest Sweden: the drainage of the Baltic Ice Lake and Younger Dryas ice margin oscillations. *Paleoceanography* **12**, 39–49 (1997).
52. Jennings, A. E., Hald, M., Smith, M. & Andrews, J. T. Freshwater forcing from the Greenland Ice Sheet during the Younger Dryas: evidence from southeastern Greenland shelf cores. *Quat. Sci. Rev.* **25**, 282–298 (2006).
53. Jakobsson, M. et al. The International bathymetric chart of the Arctic Ocean (IBCAO) version 3.0. *Geophys. Res. Lett.* **39**, L12609 (2012).
54. Leventer, A., Williams, D. F. & Kennett, J. P. Dynamics of the Laurentide ice sheet during the last deglaciation: evidence from the Gulf of Mexico. *Earth Planet. Sci. Lett.* **59**, 11–17 (1982).

Acknowledgements

We thank the officers and crew of USCGC Healy for making this project a success. We are also indebted to M. Carman for help processing core samples, A. McNichol for helpful discussions of ^{14}C in the Arctic, A. Gagnon for the stable isotope measurements, the NOSAMS staff for providing ^{14}C data and M. McCarthy, C. Moser, C. Griner and C. Mayo for leading the coring effort. S. Nielsen helped with translation of Hartz and Milthers[14]. The manuscript benefited from help from M. Blaauw and B. Keigwin with the Bayesian age model. This research was funded by NSF grants ARC 1204045 to L.D.K. and ARC 1203944 to N.W.D.

Author contributions

L.D.K. and N.W.D. conceived the project, N.W.D. and S.K surveyed the seafloor, identified coring locations and studied grain size; B.R. conducted the magnetic measurements; N.Z. and L.G. conducted the XRF scanning; and N.Z. helped develop the chronology. All the authors helped write the manuscript.

Competing interests

The authors declare no competing interests.

Additional information

Supplementary information is available for this paper at https://doi.org/10.1038/s41561-018-0169-6.

Reprints and permissions information is available at www.nature.com/reprints.

Correspondence and requests for materials should be addressed to L.D.K.

Publisher's note: Springer Nature remains neutral with regard to jurisdictional claims in published maps and institutional affiliations.

Methods

Site survey methods, laminae counting methods, core sampling and stable isotope methods, sample preparation for radiocarbon dating and Bayesian age modelling are presented in Supplementary Information sections 1, 2, 3, 4.2 and 4.4.

Data availability. Radiocarbon data appear in Supplementary Table 1, and stable isotope data appear in Supplementary Table 2. The Fe/Ca and magnetic data are available from the authors upon request. Geophysical data are available at the Lamont-Doherty Earth Observatory (https://ldeo.columbia.edu/research/databases-repositories).

Code availability. The code for the bacon age model is freely available at http://chrono.qub.ac.uk/blaauw/bacon.html. The settings used are given in Supplementary Section 4.4.